The Potential Predictability of Fire Danger Provided by Numerical Weather Prediction

Francesca Di Giuseppe, Florian Pappenberger, Fredrik Wetterhall, and Blazej Krzeminski

European Centre for Medium-Range Weather Forecasts, Reading, United Kingdom

Andrea Camia, Giorgio Libertá, and Jesus San Miguel

Joint Research Centre, Ispra, Italy

ABSTRACT

A global fire danger rating system driven by atmospheric model forcing has been developed with the aim of providing early warning information to civil protection authorities. The daily predictions of fire danger conditions are based on the U.S. Forest Service National Fire-Danger Rating System (NFDRS), the Canadian Forest Service Fire Weather Index Rating System (FWI), and the Australian McArthur (Mark 5) rating systems. Weather forcings are provided in real time by the European Centre for Medium-Range Weather Forecasts forecasting system at 25-km resolution. The global system's potential predictability is assessed using reanalysis fields as weather forcings. The Global Fire Emissions Database (GFED4) provides 11 yr of observed burned areas from satellite measurements and is used as a validation dataset. The fire indices implemented are good predictors to highlight dangerous conditions. High values are correlated with observed fire, and low values correspond to nonobserved events. A more quantitative skill evaluation was performed using the extremal dependency index, which is a skill score specifically designed for rare events. It revealed that the three indices were more skillful than the random forecast to detect large fires on a global scale. The performance peaks in the boreal forests, the Mediterranean region, the Amazon rain forests, and Southeast Asia. The skill scores were then aggregated at the country level to reveal which nations could potentially benefit from the system information to aid decision-making and fire control support. Overall it was found that fire danger modeling based on weather forecasts can provide reasonable predictability over large parts of the global landmass.

1. Introduction

Wildfire activity is strongly affected by four factors: fuels, climate/weather, ignition agents, and people (Flannigan et al. 2005). Where fuel is available, weather is the most important factor in shaping fire regimes in many areas of the world (Flannigan et al. 2009). Fires are a global phenomenon extending from the boreal forests of Canada and Siberia down to Amazonia and the central African rain forests. Especially in a savanna ecoclimate, such as the Sahel and west Australia, fires are recurrent hazards because of frequent severe drought conditions but also (as for West Africa) because of agriculture practice (Swaine 1992). Fires also occur in wetter regions such as Southeast Asia (Thailand, Malaysia, and Indonesia) mostly during the dry period before the monsoon onset.

Assessments of forest fire danger in countries with extensive forest cover have for decades relied on a combination of weather information and evaluation of the vegetation state (Taylor and Alexander 2006). Traditionally, fire danger is evaluated at observation stations where weather measurements are routinely available and vegetation status is recorded. The resulting fire danger rating is then extrapolated to a large but undefined area surrounding the observation site. Examples of systems that relay on extrapolation techniques are the U.S. Forest Service National Fire-Danger Rating System (NFDRS; Deeming et al. 1977), the Canadian Forest Service Fire Weather Index Rating System (FWI; Van Wagner 1974,

Corresponding author address: Francesca Di Giuseppe, ECMWF, Shinfield Park, Reading RG2 9AX, United Kingdom.
E-mail: digiuseppe@ecmwf.int

1987), and the Australian McArthur (Mark 5) rating systems (McArthur 1966, 1967; Noble et al. 1980). These widely used systems provide estimates of fire danger in terms of fire ignition and behavior, energy release, and rate of spread (San-Miguel-Ayanz et al. 2003).

The European Forest Fire Information System (EFFIS; Camia et al. 2006) is currently being developed in the framework of the Copernicus Emergency Management Services to monitor and forecast fire danger in Europe. The system provides timely information to civil protection authorities in 38 nations across Europe (for details, see http://forest.jrc.ec.europa.eu/effis/abouteffis/effis-network/) and mostly concentrates on flagging regions that might be at high danger of spontaneous ignition because of persistent drought. It relies on the calculation of the NFDRS, FWI, and Mark 5 matrices and uses medium-range (1–10-day lead time) weather forecasts instead of observations to extend the advance warning. For some nations and regions, case studies have already shown the advantage of such an approach: Roads et al. (2005) and Mölders (2008, 2010) used regional numerical weather inputs to drive the NFDRS system showing good prediction skill up to one season ahead, and Preisler et al. (2009) used a combination of forecast model outputs and satellite observations to extend the spatial information provided by station-based fire index calculations.

A challenge in building such a warning system is that it requires the availability of global fields such as fuel maps, vegetation characteristics, and topography. Information such as the "greenness" of the vegetation needs to be available in real time and on a global scale at the desired resolution to approximate the traditional human judgment. The quality of such an automated system will ultimately depend on two factors: (i) the accuracy of the modeling components that translate the status of the vegetation into fire danger and (ii) the accuracy of the driving fields in predicting the real atmospheric conditions. A model-based evaluation can be used to define the upper boundary of the achievable skill of such a system. This is often called *potential predictability*, and its assessment is the subject of this paper.

The driving data need to be from a homogeneous global sample to assess potential predictability, which in turn allows a global comparison of fire index calculations without dependency on forecast skill. This can, for example, be achieved by using atmospheric reanalysis. These datasets are created by combining model and quality-controlled observations for past conditions in a statistically optimal way by means of an assimilation scheme (Tang et al. 2008). A reanalysis provides a dynamically consistent estimate of the climate state at each time step and can, to a large extent, be considered as a good proxy for observed meteorological conditions. Being a model integration, it has the added benefit to also provide a dynamical set of fields, including variables that are not generally observed. How close reanalysis output is to real observations depends on the amount and quality of observations available, the accuracy of the model used, and of the assimilation scheme chosen (Dee et al. 2011). Even with these caveats in mind, fire danger indices calculated from a reanalysis dataset are less affected by uncertainties in the atmospheric forcing when compared with indices calculated from forecast fields that are the result of sole model integrations. Therefore, reanalysis fire indices can be compared with observed occurrence of fire to understand the *potential* predictability of the modeling components in detecting fire danger and ultimately to highlight the limitations of those components themselves.

In this paper we concentrate on the prediction skills of the modeling components of the EFFIS system, that is, the Global ECMWF Fire Forecasting (GEFF) model. The GEFF model provides outputs in terms of fire danger indices that are then distributed to the EFFIS network and used among the European civil protections. Although important for an operational system, we will not detail how the information produced by GEFF are translated into fire suppression actions at the European central level and in the national agencies that are part of the EFFIS network. The objective of this work is to introduce the modeling components and identify regions where the system shows high and low *potential* predictability of fire danger.

2. Methods

a. Fire danger metrics

Each of the three fire rating systems implemented into the GEFF model provides a comprehensive set of outputs that characterize different aspect of fire conditions. It is therefore important to clarify which aspect related to fire is going to be analyzed in this work. The primary scope of the EFFIS is to provide daily information of fire danger, which is intended as a general term to express an assessment of both fixed and variable factors of the fire environment that determine the ease of ignition, rate of spread, difficulty of control, and fire impact as defined by the National Wildfire Coordinating Group (http://www.nwcg.gov/term/glossary/fire-danger). Fire danger has, therefore, several components, and the rating indices chosen should be a combined metric expressing the probability of ignition, the speed and likelihood of spread, and the fuel availability (sustainability of the event).

Among all the fire indices that are outputs of the GEFF model, the FWI and the fire danger index (FDI) from the

McArthur Mark 5 system are selected as good indicators of fire danger containing both a component of fuel availability (drought conditions) and a measure of ease of spread. In the NFDRS, two indices could be used to indicate fire danger: the ignition component (IC) and the burning index (BI). Both of these indices have a component of spread and a component related to the available burning energy. Since these indices are strongly dependent on the fuel type and the local atmospheric conditions, they measure local short time variation of burning conditions as opposed to long-term danger conditions. Looking at the correlation between the BI and the IC and both the FWI and the FDI (not shown), it was found that the IC has a better correlation with the FWI and the FDI and was therefore selected as the best index within the NFDRS to compare with the other two fire danger rating systems.

In this study we limit the analysis of fire predictability to these three indices so as to provide a concise analysis of the generic fire danger predictability. Keep in mind, though, that in the actual operational implementation of EFFIS, which uses real-time forecasts as atmospheric forcings, once dangerous areas are identified, a more detailed analysis can be performed to characterize the event in terms of, for example, expected containment actions required. (In operational practice, this is usually achieved by gathering additional information provided by all of the other indices that are calculated as a part of the fire danger rating system provided in Table 2, which is described in more detail below.)

1) NATIONAL FIRE-DANGER RATING SYSTEM

In the NFDRS, the characteristics of fire danger are functions of fuel type, topography, and weather (Bradshaw et al. 1983; Cohen and Deeming 1985; Burgan 1988). The model explicitly calculates the moisture content of dead and living vegetation.

Dead fuel is divided into classes according to its fast or slow response to the changes in atmospheric temperature and humidity forcing, while live fuel is divided into herbaceous and woody shrubs. The ignition component is a rating of the probability, between 0 and 100, that a firebrand will cause a fire requiring a suppression action. Its value depends on the moisture content of the fastest responding fuel and the available fuel energy stored as a consequence of the lack of moisture in the deeper layers.

2) FIRE WEATHER INDEX SYSTEM

Similarly to the NFDRS, the FWI describes the effects of atmospheric temperature, humidity, precipitation, and wind, first on the fuel moisture content and consequentially on the fire behavior and occurrence (Van Wagner and Pickett 1985; Stocks et al. 1989). While the NFDRS allows the user to specify different fuel types, the FWI is specifically calibrated to describe the fire behavior in a standard jack pine stand *Pinus banksiana* typical of the Canadian forests (Van Wagner 1974). Despite this limitation, the index has successfully been used in countries where vegetation is dissimilar to Canada (Taylor and Alexander 2006) such as Australia (Cruz and Plucinski 2007), New Zealand, and Malaysia (Taylor and Alexander 2006) and can therefore provide useful information worldwide. In the FWI system, the fuel moisture content is calculated with different codes depending on the fuel consistency. Litter and fine fuels occupy the first fuel bed layers. Its moisture content is calculated using the fine fuel moisture code (FFMC). The moisture content of the loosely compacted organic layers of moderate depth is instead given by the duff moisture code (DMC), while the moisture of deep, compact organic layers is evaluated using the drought code (DC). From these diagnostic, weather-driven fuel moisture calculations, the FWI model calculates fire behavior indices in terms of rate of fire spread [initial spread index (ISI)] and fuel available for combustion [buildup index (BUI)]. The FWI integrates current ISI and BUI to produce a unitless index of general fire intensity.

3) MCARTHUR'S FOREST FIRE DANGER METER (MARK 5)

The McArthur's Forest Fire Danger Meter (Mark 5) was developed to monitor fire danger throughout eastern Australia. Unlike the other two indices in this model, there is not an explicit description of the evolution of moisture in different fuel types. The formulation in Noble et al. (1980) uses atmospheric conditions to evaluate a generic component representing fuel availability called the drought factor (DF). The DF is used to then calculate the FDI, which provides an assessment of fire danger due to the combined effect of drought condition and fuel availability. The drought factor is given a number between 0 and 10 and represents the influence of recent temperature and rainfall events on combustible material availability. It is partly based on the soil moisture deficit, which is commonly calculated using the Keetch–Byram drought index (KBDI; Keetch and Byram 1968), which measures the effects of seasonal drought on fire danger. The actual numeric value of this index is an estimate of the amount of precipitation needed to bring the soil back to saturation. In its original formulation, the KBDI only deals with the top 8 in. (1 in. = 2.54 cm) of the soil profile, meaning the maximum KBDI value is 800.[1] KBDI is sometimes used as a fire danger indicator in itself. Its relationship to fire danger is that as the index value increases, the vegetation is

---

[1] 8.00 in. of precipitation would be needed to bring the soil back to saturation.
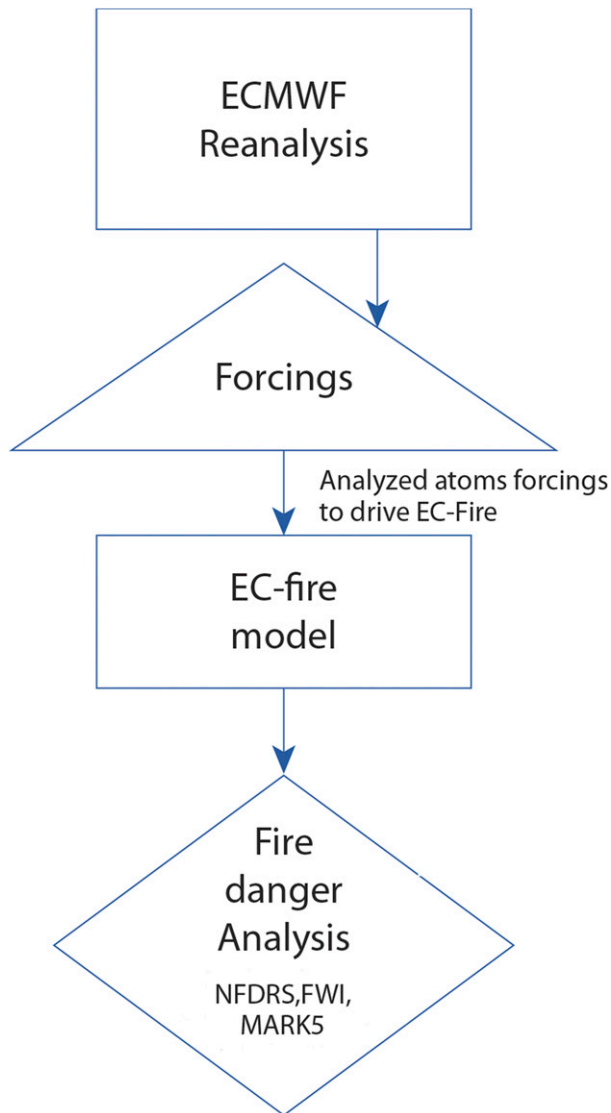
FIG. 1. Schematic of the reanalysis setup with boxes representing models, triangles showing processes, and diamonds used for products. The operational numerical weather prediction reanalysis is used to drive the GEFF model to provide an analysis of fuel moisture values and fire weather indices. All atmospheric variables undergo preprocessing before application to the fire model, which then provides analysis of fire danger indices given in Table 2, below.

subjected to increased stress due to moisture deficiency, living plants die and become fuel, and the duff/litter layer becomes more susceptible to fire (Preisler et al. 2004).

b. Fire danger reanalysis

The analysis system (Fig. 1) was designed using weather information from the ERA-Interim reanalysis system of the European Centre for Medium-Range Weather Forecasts (ECMWF) (Dee et al. 2011). ERA-Interim is the latest of the ECMWF reanalysis products and

stretches from 1 January 1979 and is extended forward in near–real time. It employs a sequential 4D-var data assimilation scheme that ensures the optimal consistency between the available observations and the model background (Courtier et al. 1994). The reanalysis data have an original spatial resolution of around 80 km and have been bilinearly interpolated to a regular latitude–longitude grid of 0.25° to be comparable with the available observational dataset of fire activity. Therefore, ERA-Interim has quite a coarse resolution and does not represent small-scale processes that might be responsible in establishing local favorable conditions for small fires. For this reason, most of the following analysis will concentrate on medium to large fire events (>2500 ha).

In addition to these daily data, the GEFF model also relies on constant fields (Fig. 2). There are three tiers of input data to the model. Tier 1 comprises the so-called climatological fields that are precomputed and kept invariant during the runs. Examples are the land–sea mask, the vegetation cover, and the orography. Tier-2 data are daily averaged fields such as 24-h accumulated precipitation, minimum and maximum daily temperature, and humidity. These are calculated from the 3-hourly outputs of ERA-Interim. Tier-3 data are atmospheric fields at a nominal 1200 local time when the condition for wildfire is most favorable. A model integration at any nominal time will simulate the atmospheric conditions at a different local time depending on the location. A temporal and spatial collage of 24-h time model simulations is performed to produce a snapshot at 1200 local time. Thus temperature and relative humidity fields are cut into 3-hourly time strips using the closest 3-h forecast output and then concatenated together so that the final field is representative of the conditions around the local noon within the 3-h resolution available. Using this method, the driving forcings are a composite of forecast outputs at different lead times in a 24-h interval and could therefore have different forecast accuracy. This inconsistency is assumed insignificant given the limited difference in forecast skills in a 24-h lead time range (Buizza et al. 1999).

The schematic in Fig. 2 shows how these three tiers of forcings are linked to the various output components of the fire index system. The summary of the data input needed is given in Table 1, while a detailed explanation of the preprocessing needed to obtain the climatological fields (tier 1) is provided in the appendix. Since the various components of the three fire rating systems are calculated from the same set of forcings, they are directly comparable. Although this work concentrates on fire danger, the system also provides a comprehensive set of fields modeling vegetation stress, probability of ignition, and fire behavior. A list of these output variables of the system is shown in Table 2.
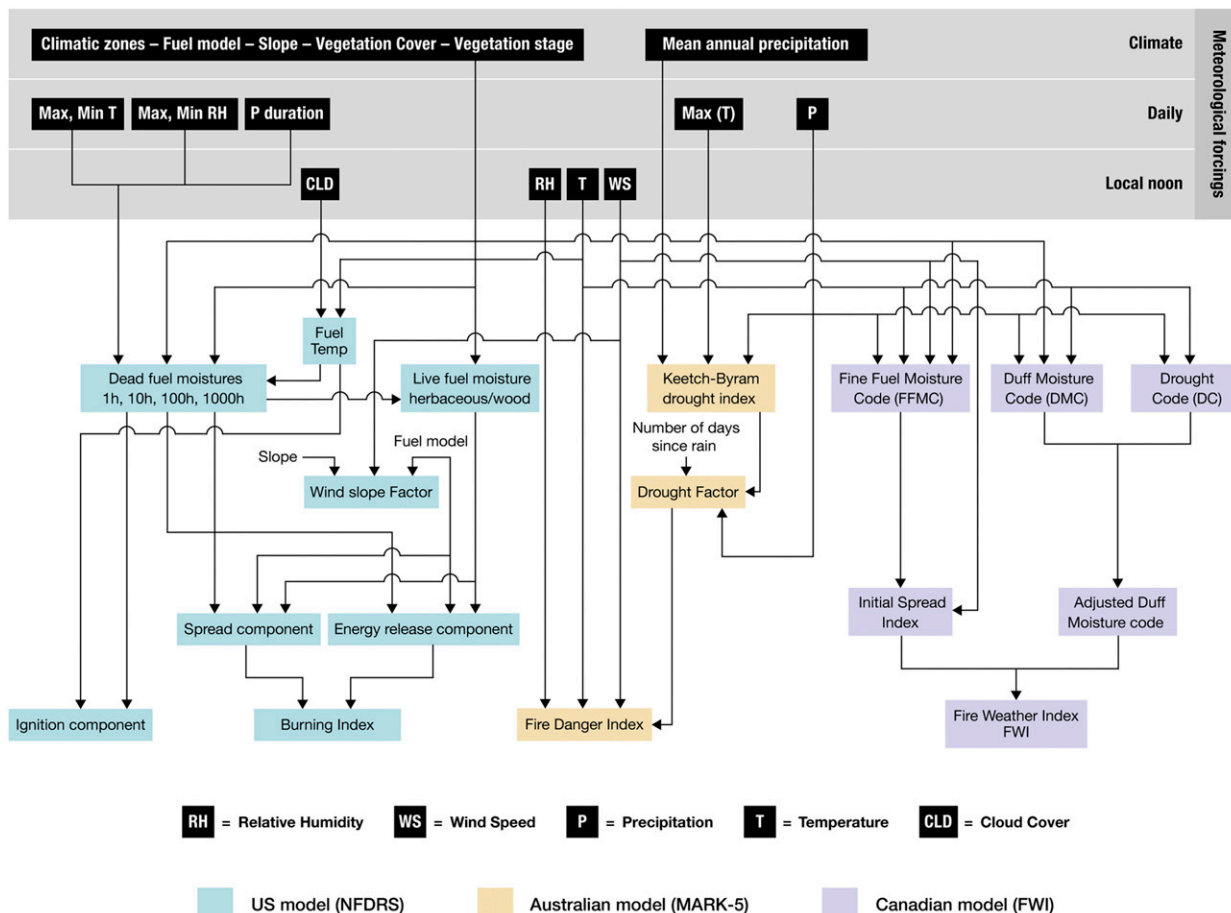
FIG. 2. Schematic of the GEFF model components with the input and output connections. Three fire danger rating systems (FWI, NFDRS, and Mark 5) are implemented using the same atmospheric forcings. Input data are grouped in three tiers: Tier-1 data are climatological fields that are precomputed and kept invariant during the runs, tier-2 data are daily averages, and tier-3 data represent instantaneous values at a nominal 1200 local time.

The reanalysis dataset for fire danger was calculated starting from 1 January 1979 and run for 36 years with a daily time step following the availability of ERA-Interim. Since the initial conditions were set using an idealized state the fire variables suffer from the so-called spinup in the first months of the forecasts as the model drifts to its own equilibrium state. The first year of simulation is therefore discarded from further analysis. The resulting fire analysis does not incorporate observations in contrast to atmospheric analysis systems.[2]

For this reanalysis, all of the fire indices were set to zero (and the moisture content of the fast-responding vegetation classes was raised to 35% in the NFDRS) if snow was on the ground or the daily precipitation is above 1.5 mm day^{-1}. Areas where vegetation fuel is not available were masked out (Fig. A6 in the appendix).

c. Observations

National inventories of wildfire activities exist in many countries (e.g., Westerling et al. 2006) but they do not have the global coverage and/or the extended record needed for a validation of a fire danger system at a global scale. Satellite observations can supply a valid alternative especially as they cover remote areas where in situ observations are sparse (Flannigan and Vonder Haar 1986; Giglio et al. 2003; Schroeder et al. 2008). Satellite data have been used to monitor biomass burning at regional and global scales for more than two decades using algorithms that detect the radiative emission from active fires

---

[2] While the FWI and Mark 5 systems are diagnostic formulations that could not benefit from the assimilation of observation, the NFDRS includes prognostic equations for the fuel moisture content that could, in theory, ingest available measurements provided an assimilation scheme were available. Nevertheless, direct observations of fuel moisture are only collected in isolated research projects thus not available at the spatial scale required for global applications.

TABLE 1. Summary of atmospheric and surface forcings input to the GEFF system.

Variable	Time	Processing	Data source–reference
Climatic zones	Invariant	Digitalization and spatial interpolation	Data from images available in Chen and Chen (2013)
Fuel model		Composite obtained from JRC	The dataset can be downloaded at http://forobs.jrc.ec.europa.eu/ products/glc2000/glc2000.php
Slope		Slope classes calculated from IFS climatological slope field	Calculated from the high-resolution GTOPO30 dataset following Baines and Palmer (1990) and Lott and Miller (1997)
Vegetation cover		Combination of high vegetation and low vegetation from IFS climatological fields	Built from the GLCC dataset described in Loveland et al. (2000)
Vegetation stage	Annual climatology	See appendix for details	Database from MODIS data (Myneni et al. 2002) processed as in Boussetta et al. (2013)
Mean cumulative annual precipitation		Annual cumulative precipitation averaged over the period 1980–2014	ERA-Interim (Dee et al. 2011)
Max/min daily temperature Max/min daily relative humidity Precipitation duration (h)	Daily value	Max, min, and number of hours calculated from the 3-hourly model outputs	ERA-Interim (Dee et al. 2011)
Cloud cover Relative humidity Temperature Wind speed	Local noon	Temporal interpolation in a 24-h forecast interval	ERA-Interim (Dee et al. 2011)

at the time of satellite overpass and in the last decade by using burned area algorithms that directly map the spatial extent of the area affected by fires (Wooster et al. 2003; Giglio et al. 2006).

The burned area dataset of the Global Fire Emissions Database (GFED4) combines several satellite products in a homogeneous time sequence of events (Giglio et al. 2013) from August 2000 to the present. Among estimations of fire emission, it provides daily burned area fraction with a 0.25° resolution. GFED4 combines 500-m MODIS satellite burned area maps with active fire data from the Tropical Rainfall Measuring Mission (TRMM)

TABLE 2. Summary of outputs available from the GEFF system. The indices used in this paper are in boldface type.

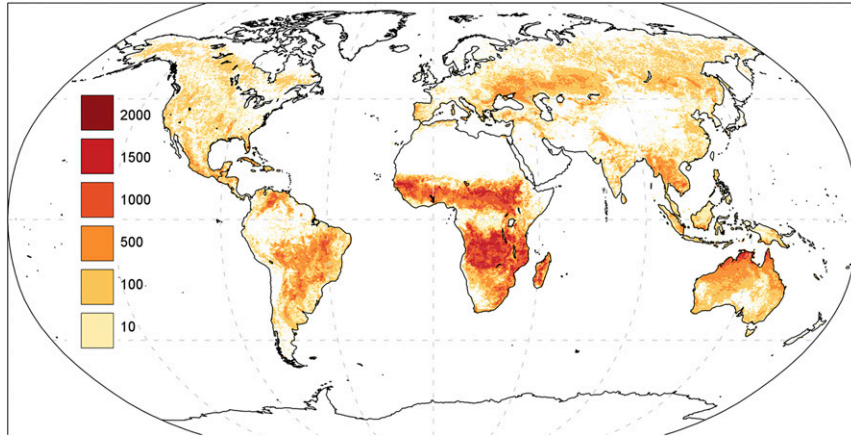| Rating system	Variable	Description
FWI	Fine fuel moisture code (FFMC)	Numerical rating of the moisture content of litter and other cured fine fuels.
	Duff moisture code (DMC)	Numerical rating of the average moisture content of loosely compacted organic layers of moderate depth.
	Drought code (DC)	Numerical rating of the average moisture content of deep, compact organic layers.
	Initial spread index (ISI)	Numerical rating of the expected rate of fire spread.
	Buildup index (BUI)	Numerical rating of the total amount of fuel available for combustion.
	Fire weather index (FWI)	Numerical rating of fire intensity. It is suitable as a general index of fire danger.
Mark 5	Keetch–Byram drought index (KBDI)	Metric of seasonal drought severity and fuel availability.
	Drought factor (DF)	Metric of fuel availability as determined by seasonal severity and recent rain effects.
	Fire danger index (FDI)	Numeric rating related to the chances of a fire starting, its rate of spread, its intensity, and its difficulty of suppression.
NFDRS	Spread component (SC)	Forward rate of spread at the head of the fire in feet (1 ft = 30.5 cm) per minute.
	Energy release component (ERC)	Potential available energy at the head of the fire.
	Ignition component (IC)	Numerical rating of the probability that a fire that requires suppression action will result if a firebrand is introduced into a fine fuel complex.
	Burning index (BI)	Metric of flame length in feet at the head of a fire.

FIG. 3. Number of active fire days recorded in the GFED4 dataset during the 4900 days covering the period from August 2000 to December 2013.

Visible and Infrared Scanner (VIRS) and the Along-Track Scanning Radiometer (ATSR) family of sensors. The daily burned area dataset is used in this paper to validate the relationship between the modeled fire danger and the observed occurrence of fire episodes. Fire events are defined when the burned area fraction is larger than 0.1 (10% of the pixel area). Considering the resolution of the dataset, this choice implies that we "activate" a cell when fires have an extent of at least $2.5 \, \text{km}^2$ (2500 ha). Hantson et al. (2015) show that fire size follows a negative power-law distribution. Large fires ($>10^4 \, \text{ha}$) are orders of magnitude less frequent than small ones ($<10^2 \, \text{ha}$). Since the fire mask is constructed on fires larger than 2500 ha in our analysis, we neglect events smaller than this size, which are the most frequent. On the other hand, note that ERA-Interim has an original resolution of 80 km and it is then interpolated on to a 25-km resolution to be comparable with the observed dataset. Therefore, small-scale conditions that can impact fire danger at the local level are not explicitly represented by the weather forcings used. The prediction of fires at these unresolved scales could prove challenging. To understand the impact of fire sizes on the overall prediction skill of the system, another mask is created that takes into consideration only fires smaller than $2.5 \, \text{km}^2$ by defining the mask when the condition $0 <$ burned area < 0.1 is met. (This mask for small size fires will be used only for the generation of Fig. 9, which is described below).

Figure 3 shows the number of observed fire days during the 4900 days covering the period August 2000 to December 2013. All fires are included, even the ones induced by human actions, which, despite requiring favorable climatic conditions to be sustained, are not explicitly modeled by the fire indices algorithms used in this paper.

d. Normalization

The three indices exhibit different ranges of values, which makes a direct comparison difficult and presents a barrier to integrate this information in an early warning application. The global cumulative distribution function (CDF) for all values above zero in the 11 yr from August 2000 to December 2013 is shown in Fig. 4. It shows, for example, that FWI ≥ 40 occurs in only 20% of the cases while for the same value a frequency of 5% of the cases for the Mark 5 FDI and NFDRS IC is estimated.

To make the numerical values of the indices directly comparable a transformation is performed on the raw index value $\mathcal{I}_{\text{raw}}$ to obtain a normalized index $\mathcal{I}_{\text{norm}}$. This is simply done by means of the inverse of the CDF function:
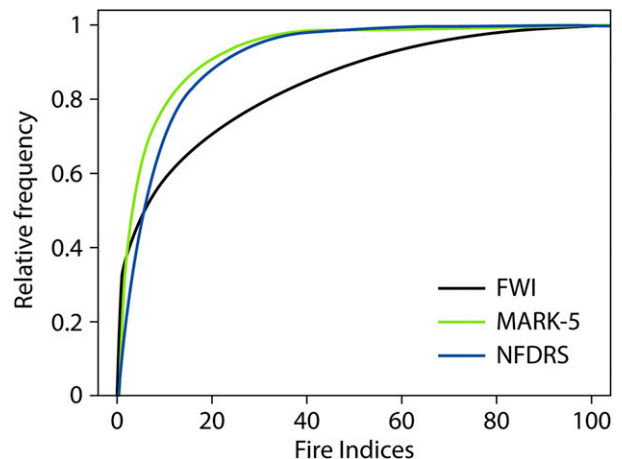

FIG. 4. CDF collecting all cases above 0 for the three indices. For any value X of a given index, the CDF represents the total number of cases for which the index was smaller than X. For example, FWI ≥ 40 occurs in only 20% of the cases.
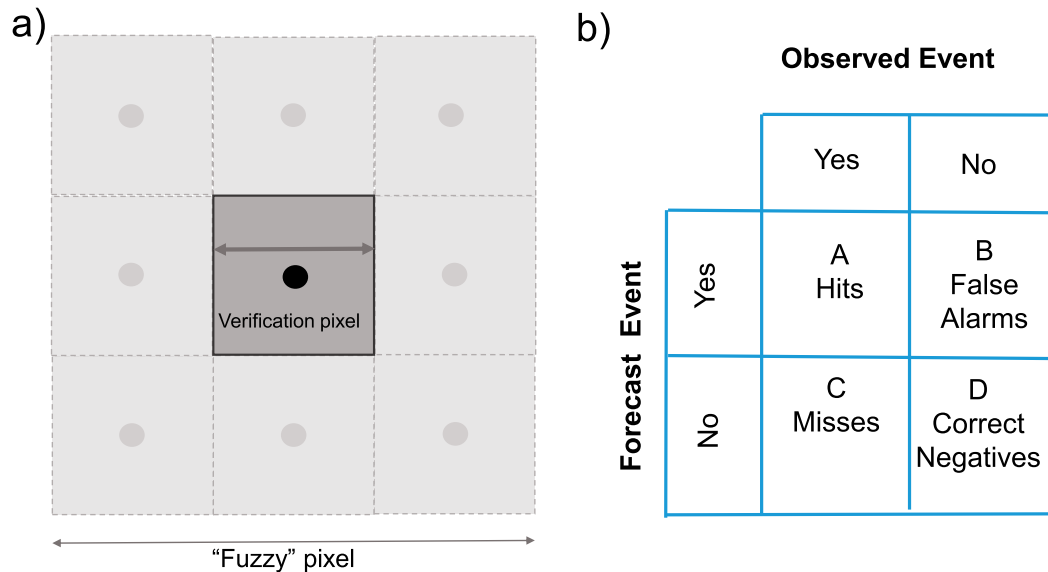
FIG. 5. (a) A graphical representation of the fuzzy logic that is applied in the verification analysis. The enlargement around the verification pixel is designed to take into account the value of a correct forecast that is offset spatially from the original verification pixel. A unique contingency table is constructed using the nine pixels instead of only the verification pixel. This means that any hits in the neighborhood will count toward enhancing the EDI value in the verification grid box. (b) Contingency table used for the verification of binary events (occurred/did not occur). The numbers of observed and predicted events in any of the four categories (hit, miss, false alarm, and correct negative) are used to derive skill scores.

$$\mathcal{I}_{\text{norm}} = \text{CDF}_{\mathcal{I}}^{-1}(\mathcal{I}_{\text{raw}}). \tag{1}$$

In this way, all indices are normalized over [0, 1] using the maximum and minimum (above 0) computed over all days of the available time series. Note that Fig. 4 represents a global mean and has been reported for documentation purposes only. At a single site these curves might be different since they the range of possible fire danger conditions for that location.

e. Verification methods

1) DISCRIMINATION SKILL

The IC, FWI, and FDI provide information on the severity of drought conditions and the availability of fuel and thus the probability of spontaneous ignition occurrence. The numerical value should be interpreted probabilistically meaning that high values are no guarantee of actual fire occurrence. A desirable quality for the purposes of fire action planning for any system is its capability to discriminate between fire occurrence and nonevents. Therefore, one would expect high values of the indices to predict fire and low values otherwise. This information can be gathered using a discrimination diagram, that is, plotting the conditional distributions of the forecasts. For binary events (fire/no fire), this diagram plots the conditional distribution of the forecasts given that the event occurred and the conditional distribution of the forecasts given that

the event did not occur. Ideally, the two distributions should be separated from one another, becoming two distinct spikes for perfect prediction.

2) FIRE DETECTION SKILL

The calculation of fire detection skill has to take into consideration that fires are events with a low frequency (rare events) (Coles et al. 1999; Ferro 2007; Ferro and Stephenson 2011). The assessment of the quality of the prediction is therefore complicated by the fact that measures of forecast quality typically degenerate to trivial values as the rarity of the predicted event increases (Coles et al. 1999). This is easily understood by considering the contingency table for the observed and predicted fire events in Fig. 5b. Once the occurrence of the event is defined for the forecast (e.g., when $\mathcal{I} \geq$ 4th quartile) it is possible to count the number of hits (A), misses (B), false alarms (C), and correct negatives (D) in comparison with what was observed. The resulting table can then be used to derive classic skill scores such as the probability of detection POD = $A/(A + C)$, or the Brier score BS = $(A + B)/(A + C)$, to name just two. Coles et al. (1999), Ferro (2007), and Ferro and Stephenson (2011) showed how these common skill scores tend to vanish as the base rate of observed events $(A + C)/(A + B + C + D) \rightarrow 0$ regardless of the actual forecast skill. Stephenson et al. (2008) and Ferro and Stephenson (2011) proposed a series on nonvanishing

measure for rare events. The extremal dependency index (EDI) is less dependent on the base rate and more difficult to hedge [see Ferro and Stephenson (2011) for an extensive discussion on the EDI properties]. EDI provides a skill score in the range $[-1, 1]$. EDI takes the value of 1 for perfect forecasts and 0 for random forecasts. It is >0 for forecasts that have hit rates that converge to 0, and slower than those of random forecasts, and can be negative in the opposite situation. Therefore, the system beats a random forecast for values > 0 and could be considered skillful.

3) FIRE LOCALIZATION

The accuracy in the localization of an event might not be the most important aspect for an early warning system. High fire danger forecast in the neighborhood of an observed event still adds useful information for the scope of emergency planning and should therefore be positively rated. To take this aspect into account the prediction score calculation follows a fuzzy approach using a spatial filter that aggregated a matrix of 3×3 neighboring pixels around the verification point (Fig. 5a). One contingency table is created from the nine time series. This means that any hits in the neighborhood will count toward the EDI value in the verification grid box.

3. Results

a. Comparing indices

The combined probability density function of any index combination (Fig. 6) shows the different behavior of the FWI, Mark 5, and NFDRS systems. The FWI and FDI variables are calibrated to represent the inflammability of a specific vegetation condition (i.e., boreal forest). Conversely, the NFDRS explicitly represents the evolution of the vegetation moisture content in different ecosystems, specifically the 20 fuel moisture classes given in Table 3. The ignition component of the NFDRS is calculated for different vegetation regimes and is then compared with the two other indices representing a constant vegetation. This difference is probably responsible for the larger spread in the joint probability function observed when NFDRS is used. The contour lines show the same probability density function but using a reduced dataset where at least one fire event was recorded in the GFED4 dataset (see Fig. 3). Apart from the need of rescaling, the indices show a very good correlation among each other when a linear model is used to calculate the correlation coefficient r. This proves that overall they are representative of the same phenomenon.

b. Global predictability

The potential predictability evaluates the capability of the system to effectively flag regions and periods as at
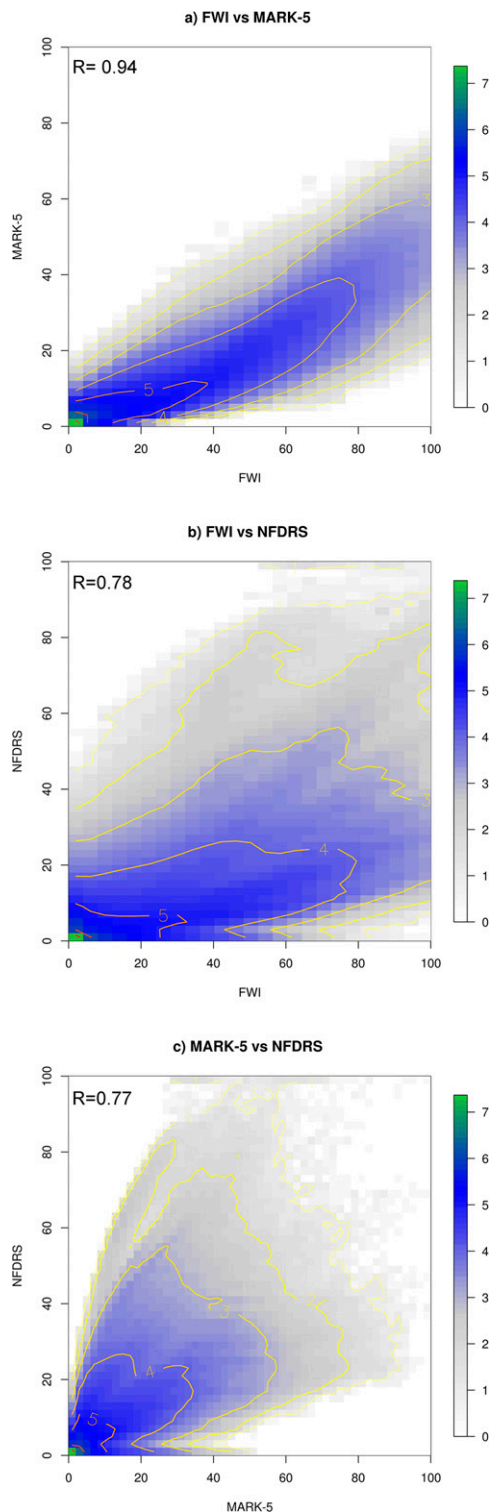

FIG. 6. Two-dimensional probability density functions for the fire danger indices implemented: (a) FWI vs Mark 5, (b) NFDRS vs FWI, and (c) NFDRS vs Mark 5. Shaded colors are used for all points in the dataset, while contour lines are used for a reduced dataset that includes only where at least one fire event was recorded in the GFED4 dataset. The sharper the distribution and the higher the regression coefficient R are, the closer is the agreement between the two indices.

TABLE 3. List of fuel types used for the NFDRS and whose geographical location is given in Fig. A6, described in more detail in the appendix.

A	Western annual grass
B	Chaparral
C	Pine grass savanna
D	Southern rough
E	Hardwood litter
F	Intermediate brush
G	Short needle, heavy dead
H	Short needle, normal dead
I	Heavy slash
J	Intermediate slash
K	Light slash
L	Western perennial grass
N	Sawgrass
O	High pocosin
P	Southern pine
Q	Alaska black spruce
R	Hardwood litter, summer
S	Tundra
T	Sagebrush–grass
U	Western pines
Water	Water
Barren	Barren
Marsh	Marsh
Ice	Snow and ice
Urban	Urban
Agriculture	Agriculture
No Data	No data

high (low) danger when actual fire events (nonevents) were observed. The discrimination diagram in Fig. 7 shows the conditional distributions of the forecasts whether the event did or did not occur. If the two distributions are well separated, the indices have a good discrimination capability and the information can be useful in an early warning system. Only two distinct spikes would be present in the case of a perfect forecast.

In roughly 80% of the cases, the indices are able to flag as above normal (i.e., >50% of climatological value) cases that developed in fire events and flag as below normal (i.e., ≤50% of climatological value) situations that did not develop into fire events. Remarkably, all the fire indices are also able to predict more severe events. A fire developed 60% of the time in which values were in the upper percentile (above 75% of all cases). FWI and Mark 5 are extremely similar in their statistical behaviors because of the similar nature of the modeling components. The IC is slightly more cautious in predicting fire events but, in contrast to the other indices, provides a lower false-alarm rate.

c. Regional fire danger detection

The global assessment in the previous section is useful to gain an appreciation of the average potential capability of the system. A regional analysis is necessary to understand in which countries/regions the automatic system has enough predictive skill to be useful to plan fire control actions. The regional analysis is performed using the fuzzy pixel logic described before. Two verifications are performed when forecast events are defined for the index being larger than the first upper quartile (≥50%; Fig. 8): 1) using the standard fire mask (fires > 2500 ha) and 2) using the fire mask for small fires only (Fig. 9).

Figure 8 shows that the predictions are very good in regions of the planet covered by boreal forests (taiga ecosystems that cover nations such as Russia, Canada, and the Nordic countries). Since the boreal forest zone consists of a mixture of conifers (white and black spruce, jack pine, tamarack, and balsam fir) it is not surprising that the FWI performs best among the indices in these areas as it is specifically calibrated for this vegetation cover. Prediction skill is higher in the Canadian boreal shield west ecozone (Stocks et al. 2002) where large fires occur frequently when compared with the Canada's montane cordillera ecozone (Stocks et al. 2002) where fires are numerous but tend to be smaller. Northern boreal Eurasia and Siberia in particular present a very
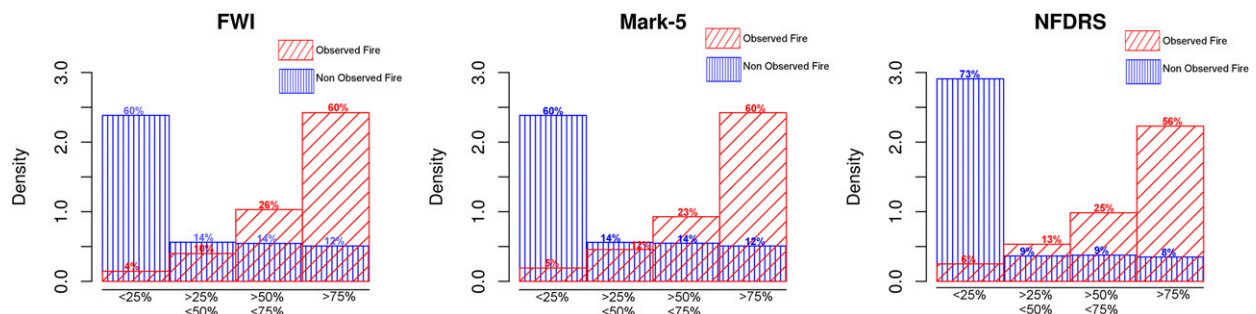

FIG. 7. Discrimination diagrams for the three indices showing the probability of the index being in any of the four quartile intervals when a fire event occurred (red histogram) and when it did not (blue histogram). Only two distinct spikes would be present in the case of a perfect forecast.
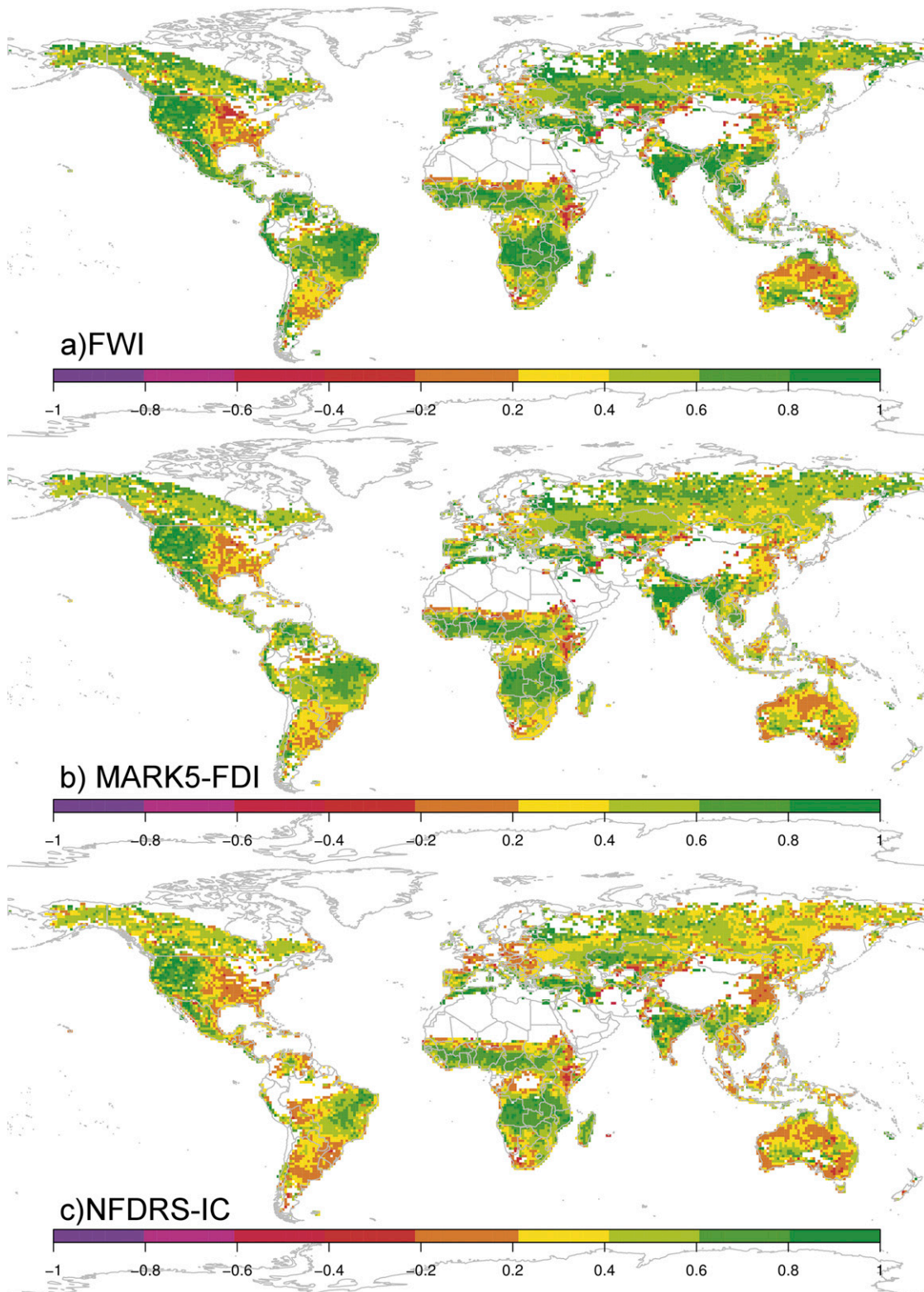
FIG. 8. EDI for the three rating systems. The EDI skill score is calculated using the fire mask derived from the GFED4 dataset. A fire is forecast when the corresponding index value is above the first upper quartile (≥50%) of its distribution. The verification contingency table (Fig. 5b) for the EDI is calculated considering the spatial fuzzy analysis depicted in Fig. 5a, which provides a 3 × 3 pixel spatial smoothing. Therefore, while the analysis is performed on the original grid of 25 km, the effective resolution is 75 km. EDI takes a value of 1 for perfect forecasts and 0 for random forecasts. Therefore, the system beats a random forecast for values above 0 and could be considered to be skillful.
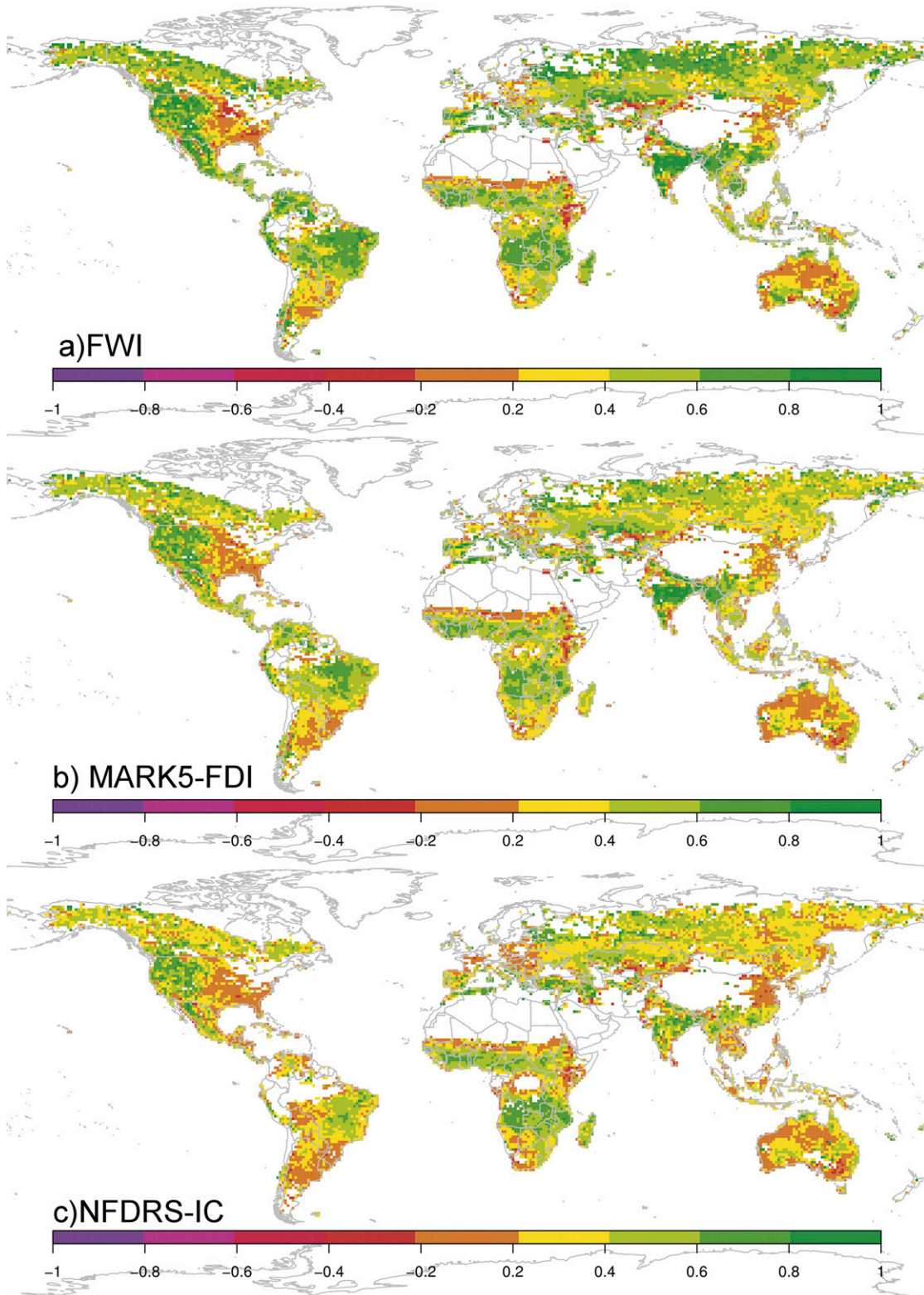
FIG. 9. As in Fig. 8, but focusing only on small fire events (<2500 ha).

similar range of fire weather conditions as in boreal Canada. In these regions the vegetation is quite homogeneous and the values of the indices are controlled mostly by the weather forcings. It has to be noted, though, that fire regimes can be very different, with the Siberian fires tending to be not as large as in Canada, relatively frequent, and having moderate to high intensity (de Groot et al. 2013).

In Australia, fires can develop in two very different environments. They can either burn in mountainous or alpine areas, which are usually densely forested, or they can start along flat plains or areas of small undulation, predominantly covered in grasses or scrubland. In the first case fire episodes can be extremely intense and long lived, while in the second case fires move quickly, fueled by high winds in flat topography, quickly consuming the small amounts of fuel/vegetation available (Bradstock et al. 2002). The predictive skill of the GEFF system seems to be able to distinguish between these two regimes and performs better in forested areas. Indeed, Luke and McArthur (1978) suggest a modification of the FDI index for grassland that could improve the prediction in this ecoclimate, although it is not implemented in the GEFF system.

Fires in Southeast Asia—comprising the countries of Thailand, Malaysia, and Indonesia—are usually human caused for the purposes of gathering nontimber products and agriculture or, as in Indonesia, due to deforestation for establishing plantations. The fire seasons in this region are controlled by rainfall seasonality associated with the monsoon, which produces an annual, or in some regions semiannual, wet–dry cycle. The NFDRS system requires quite an accurate knowledge of the vegetation cycle. Vegetation green-up and curing are, in the original implementation, human triggered, while in GEFF they are read from a mean climatological database (see the appendix). This highlights the shortcoming of a global implementation for a model that highly relies on local knowledge. The NFDRS would probably be much more locally accurate if real-time data for the vegetation stage were to be provided.

In the Mediterranean region, vegetation is dominated by a combination of shrublands and low forests. Persistent dry climatic conditions in summer favor the establishment of intense fire seasons that are only limited by the availability of fuels (Pausas and Paula 2012). Despite the different types of vegetation than are found in the boreal forests, all the indices perform remarkably well in marking fire events in these ecosystems, especially in the southern part of Spain, Greece, and Italy. The climate in Central Europe is subcontinental temperate, and the vegetation is characterized mostly by deciduous broad-leaved forests. The peak of the fire activity tends to be just after snowmelt and before leaf flushing and is driven more by short-term dryness of surface soil layers than long-term drought (Wastl et al. 2013). The potential predictability of fires is lower than in the Mediterranean region.

Finally, the large forests of South America and central Africa are characterized by large seasonal fires mostly initiated by agricultural burning. The peak of the fire season is between August and September, which coincides with the end of the dry season. Given the vast availability of fuel, the main cause of fire danger is the establishment of drought conditions, which are well predicted by all indices.

The global analysis in Fig. 8 is repeated using the mask for small fire (Fig. 9) to highlight that the EDI skill score is degraded everywhere on the planet by about 20% on average. The coarse resolution of ERA-Interim cannot resolve small-scale variations in the weather parameters that might result in the development of smaller fires. The relationship between weather anomalies and fire events is therefore weakened.

d. Aggregation at country level

EFFIS (Camia et al. 2006) has been designed with the main aim of providing decision support for the management of fire danger at European and national level. Wildfires are clearly a cross-border phenomenon, but for decision-making support, an aggregation of forecast skill to a national level can be useful to understand in which nation GEFF products could also be employed. For every nation, Fig. 10 shows the surface that was affected by at least one fire during the observational period as a percentage of the nation's ground area. The country inventory and the surface-area data are taken from Esty et al. (2008) and are not available for a few nations such as Afghanistan and Serbia. For very small countries such as Denmark and Belgium, the coarse 25-km^2 resolution of the observed dataset can also lead to misleading overestimations of the percentage of burned area. Fires might have occurred with smaller extent but are then aggregated to a larger grid at the resolution of the dataset and in some cases the grid is too coarse to "resolve" small nations. However, for most of the countries, the plot provides a reliable measure of representation by providing system skill at a country level. For very low coverage (≤10% of the country surface), the given average fire index skill might not be a meaningful indication of the real performance of GEFF in that country. This is especially true for nations with very heterogeneous vegetation covers and fire activities.

Figure 11 shows the mean skill of the three fire rating systems aggregated at a country level. Keeping in mind the information provided by Fig. 10, it shows that the
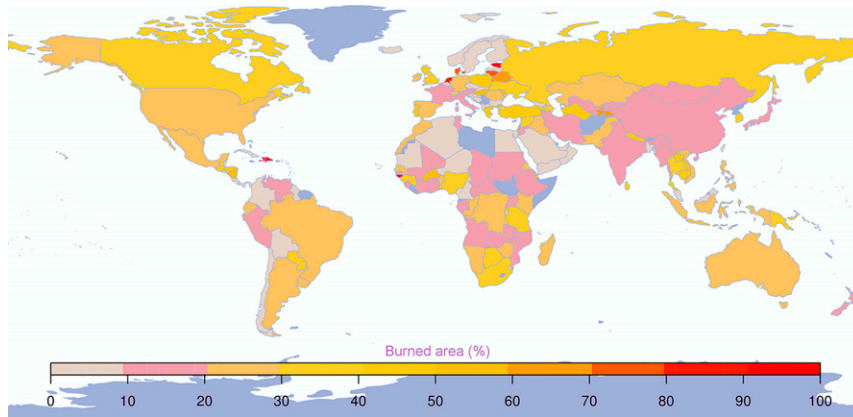
Fig. 10. Percentage of a country's surface that was affected by at least one fire during the observational period. Gray shading indicates countries for which surface-area information is missing (e.g., Afghanistan and Serbia; Esty et al. 2008).

system is able to beat the random prediction in almost all nations. All indices perform better where fire is moisture limited, such as the boreal forests, where fires are fuel limited (e.g., in the savanna).

4. Conclusions

In this paper, we have presented an operational global fire danger system that relies exclusively on forcings from atmospheric modeling. The Global ECMWF Fire Forecasting system was developed from the collaboration between the European Joint Research Centre (JRC) and the ECMWF. GEFF is the modeling component of the European Forest Fire Information System (Camia et al. 2006), which is being developed in the framework of the Copernicus Emergency Services to provide a platform of shared information on fire danger to civil protection authorities of 38 nations across Europe. GEFF calculates daily prediction up to 10 days ahead of all the indices from the U.S. Forest Service NFDRS, the Canadian Forest Service FWI, and the Australian McArthur (Mark 5) rating systems using the ECMWF forecasting system as the atmospheric forcings.

This study introduced the modeling components of the GEFF system and has assessed its maximum potential skill to identify conditions of fire danger. To this end the analysis has employed meteorological forcings from the latest ECMWF reanalysis dataset (Dee et al. 2011), ERA-Interim, instead of the more uncertain forecast fields. Reanalysis products can still be biased relative to observations, but they have the advantages over raw weather station data by providing spatially and temporally continuous records consistent with the physical constraints imposed by a numerical weather

prediction model and an optimal data assimilation algorithm. Reanalysis fire indices can therefore be compared with observed occurrence of fire to understand the *potential* predictability of the modeling components and where GEFF could provide useful information for fire control. The analysis has been performed interpolating the original 80-km ERA-Interim grid to a regular latitude–longitude grid of 25 km to match the available burned area dataset. ERA-Interim has therefore quite a coarse resolution and does not represent small-scale processes that might be responsible for establishing local favorable conditions for fire danger. For this reason, the comparison has been limited to medium to large fire events ($\geq$2500 ha).

In large areas of the planet all of the selected indices from the three fire danger rating systems are able to identify dangerous conditions for fire events. Where fuel availability is not limited—such as in the boreal forests, the Mediterranean region, South America, and central African regions—fire events are mainly controlled by persistent drought conditions, and GEFF prediction skill is high (well above the random forecast). Conversely, in temperate regions, such as the mountainous regions of Central Europe, fuel availability is limited. Here fire can depend on highly stochastic conditions, such as the short-term superficial drying of the available organic matter on the ground. In these conditions, the skill of the system degrades although it is still above the skill of a random forecast because of the small-scale nature of the processes involved.

The FWI and Mark 5 FDI indices have very similar behavior and seem to outperform the NFDRS IC index in some regions of the planet. It is fair to recall that while the FWI and FDI only rely on weather inputs
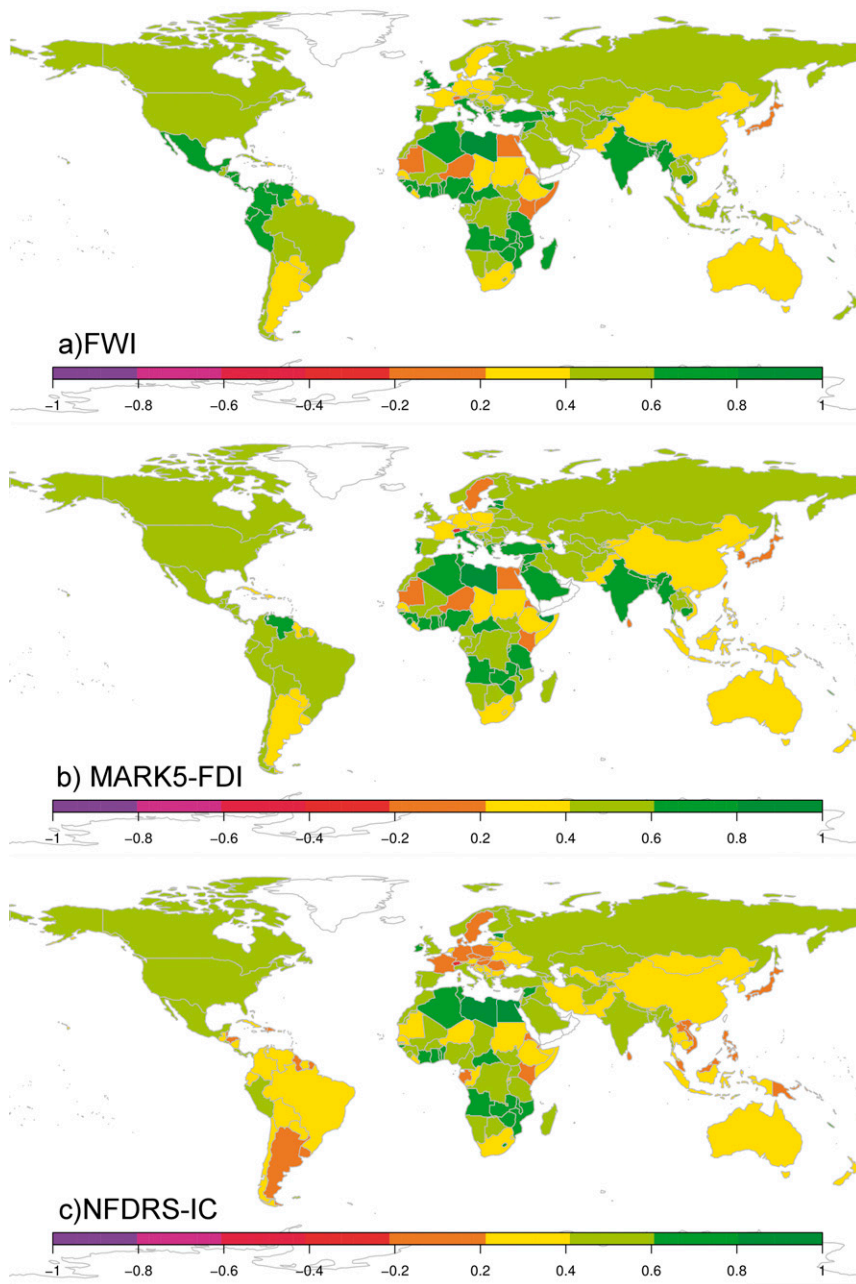
FIG. 11. EDI for the three rating systems as in Fig. 8 but averaged at the country level using the shapefiles for country borders that were defined in Esty et al. (2008).

for their calculations, the IC highly depends on the knowledge of fuel conditions such the vegetation state and its annual cycle. This information has been provided in a mean climatological way and might not be accurate enough to exploit the potential for this index. Since the GEFF system is intended to provide information on a regional to global scale, some compromises had to be made, the most important being the substitution of human judgment with mean climatological conditions for the vegetation evolutions that penalized the NFDRS system.

The very promising results show that climate model simulation may usefully extend the early warning available from environmental monitoring. It is important to emphasize that this study is a first step and is limited to identifying the potential skill in such a
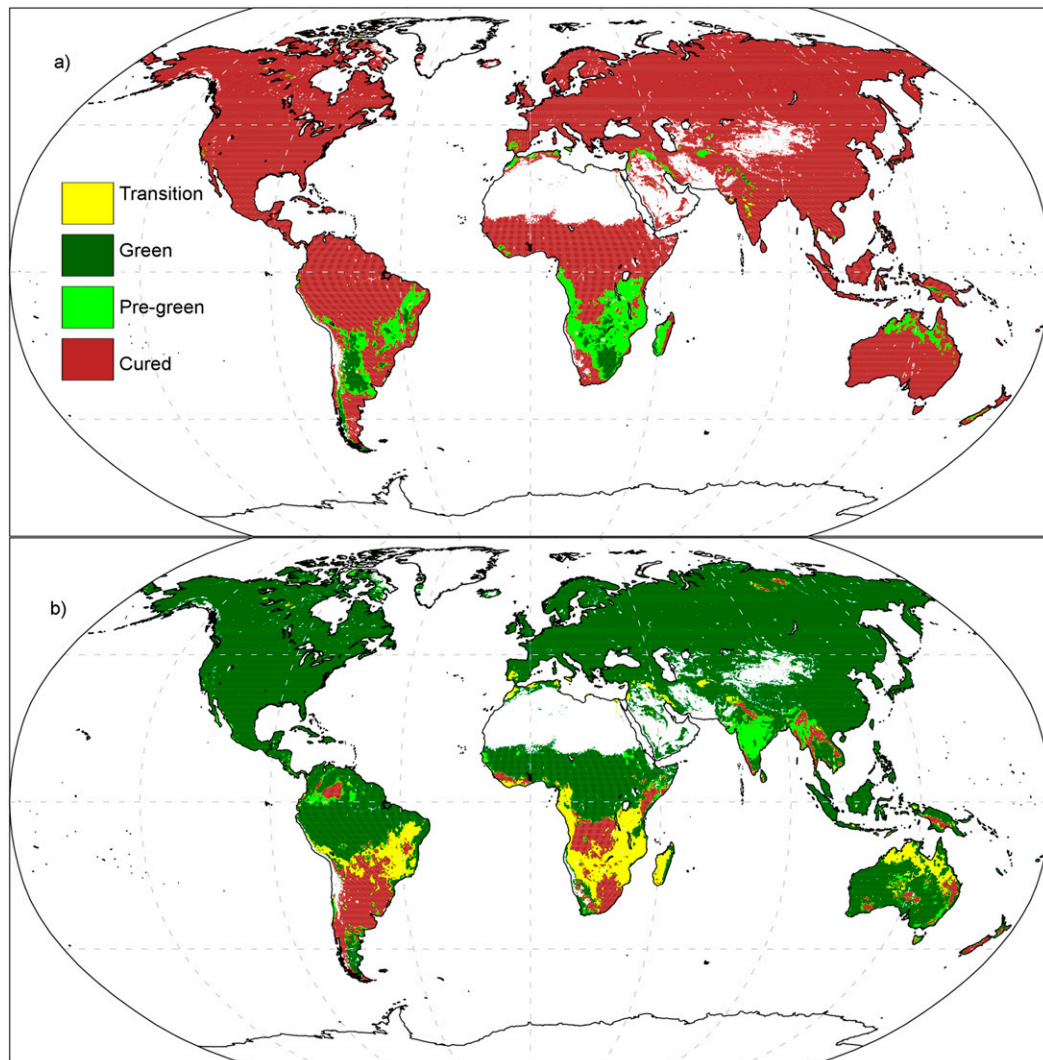
FIG. A1. Global maps of climatological vegetation stages for (a) 1 Jan and (b) 1 Jul. This dataset is derived starting from observations of LAI recorded by MODIS, applying a low-bandpass filter to remove the subseasonal variability and analyzing quartile values.

system. Actual skill of the operational forecasts extending up to 10 days will be lower because of the use of more uncertain weather forcings. In another sense, the assessment also represents a lower threshold of potential skill, since improvements in the forecast modeling systems will increase skill over time. A full analysis of the prediction skill will be the natural next step.

APPENDIX

Invariant Fields in the GEFF System

a. Vegetation stages

An annual climatology of vegetation stages is derived starting from observations of leaf area index (LAI) recorded by the MODIS instrument (Myneni et al. 2002). LAI is defined as the one-sided green leaf area per unit ground area and has been used in land surface
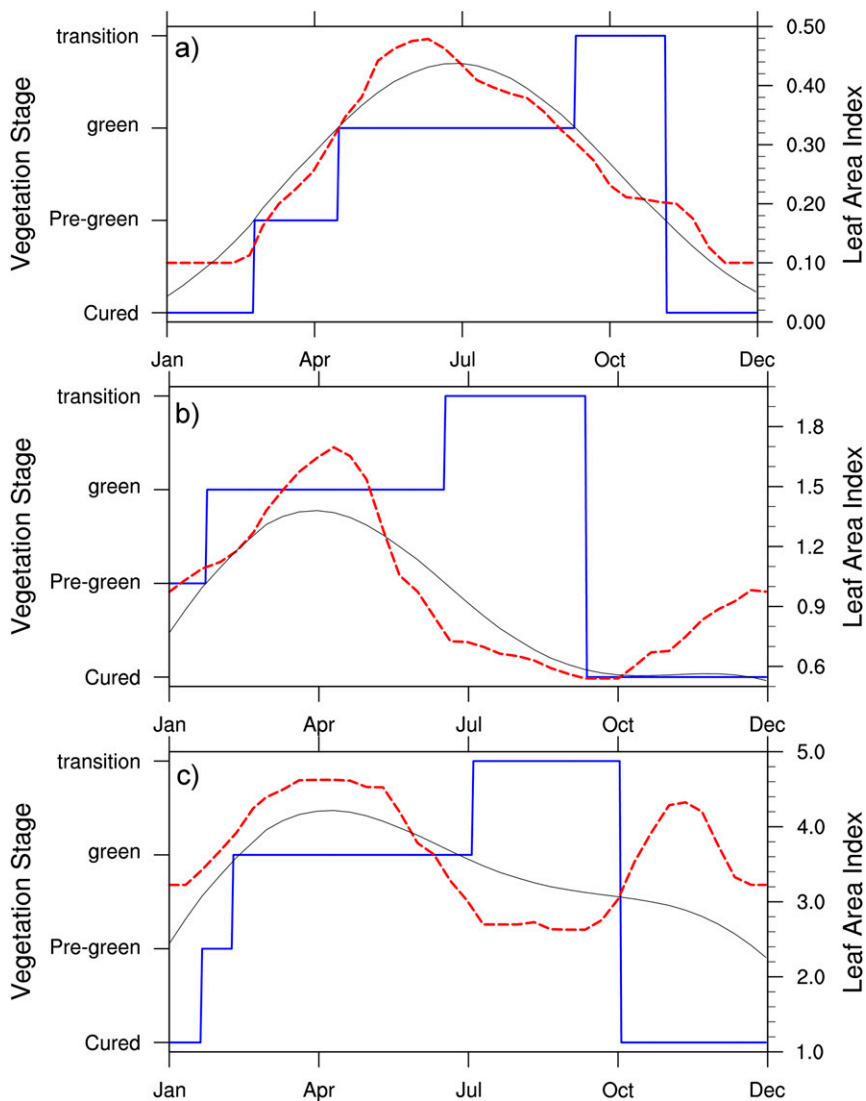
FIG. A2. Annual variability for the vegetation stage dataset in three selected locations: (a) United States (39.75°N, 115.75°W), (b) Europe (39.15°N, 7.65°E), and (c) East Africa (0.25°S, 14.55°E). The original LAI climatology (red dashed line) is smoothed with a low-bandpass filter (black solid line) to remove variability below the seasonal scale. Then the quartiles of the curve are analyzed to define the daily status among the four vegetation stages.

modeling as an indicator of the vegetation state (green-up, green, transition, and curing processes) (Knote et al. 2009). The dataset used here has been processed from the products MOD15A2 and spans the period 2000–13 with a time resolution of 10 days, as described in Boussetta et al. (2013). Quality control and temporal and spatial aggregation have been performed on the original MODIS data to generate an annual climatology of LAI that is now employed operationally as climatological LAI field in the ECMWF's integrated forecasting system (IFS) model (Boussetta et al. 2013).

Starting from this LAI dataset, we have calculated vegetation stage intervals (examples for two days are

shown in Fig. A1). For each location a low-bandpass filter is applied to the LAI climatological annual cycle to remove data variability at scales lower than the seasonal. The resulting curve is processed in terms of quartiles. Days with LAI values larger than the upper quartile are marked as ''green,'' while days with LAI value lower than the lower quartile are flagged as ''cured.'' All days remaining are checked against the derivative of the LAI annual curve. If a point belongs to the up-slope part of the curve (i.e., positive derivative) it is then flagged as ''pre-green,'' otherwise it is marked as ''transition.'' This approach leads to very realistic climatological vegetation stage in locations where vegetation is characterized by a
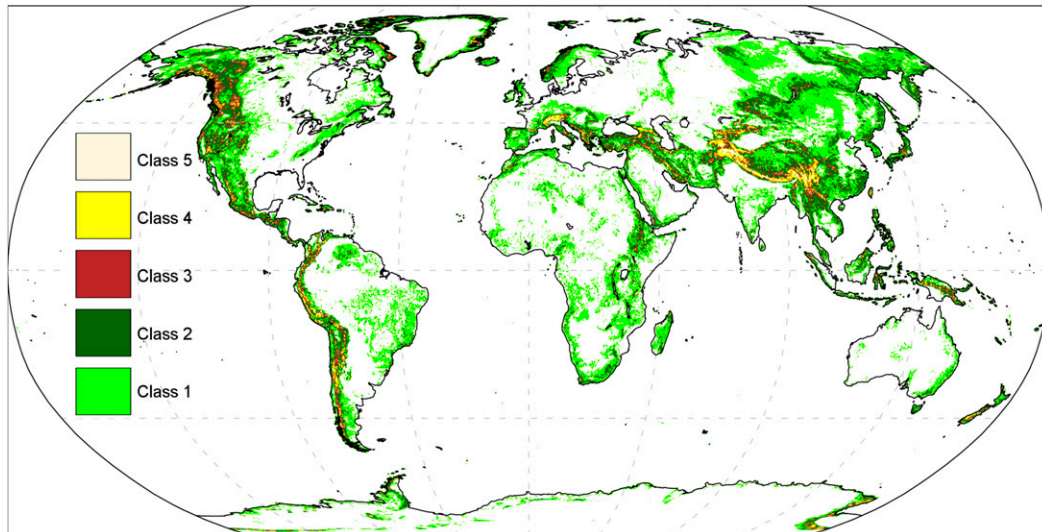
FIG. A3. Slope classes derived from the IFS model slope field.

clear annual cycle. In the extratropics where precipitation is associated with frontal systems and is in general seasonal, this is usually a good approximation (Figs. A2a,b). In other regions, mostly in the tropics where precipitation is driven by, for example, monsoon systems, a single peaked annual vegetation cycle might not represent fully the interannual variability. In East Africa, for example, there are two monsoon-driven rainy seasons. They are responsible for two germination phases in spring and autumn (Fig. A2c). Only the green-up and green phases associated with the long rain in April are picked by the

automatic procedure after the filter smoothing. From the point of view of the fire danger assessment, this limitation of the system in local points is nevertheless deemed acceptable since it goes in the direction of increasing the false alarms while underestimating the missed events.

b. Orographic parameters

The model orographic parameters needed to initialize GEFF are taken from IFS model's invariant fields for consistency. The orography is based on an interpolated version of the terrain elevation dataset GTOPO30 at 30-s
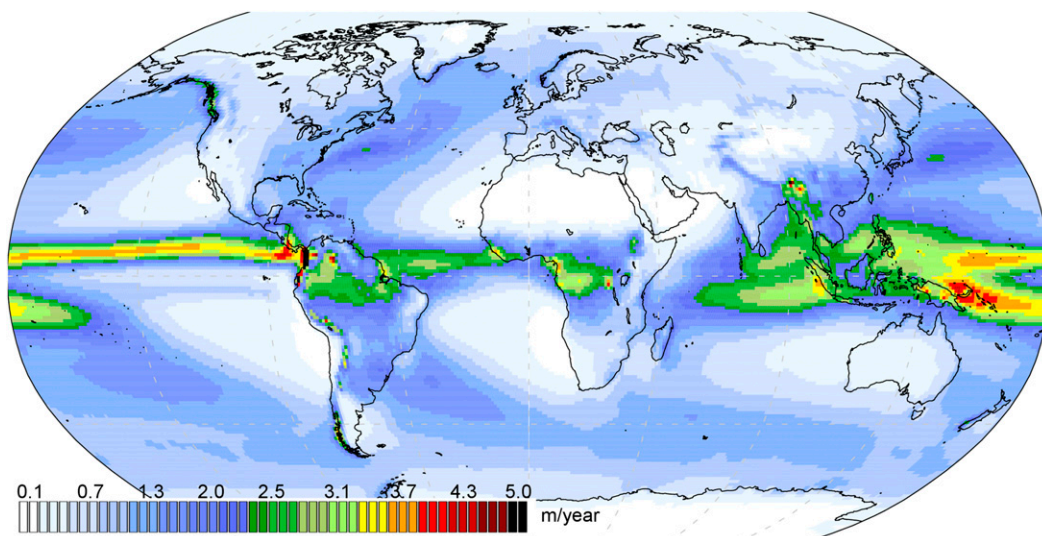

FIG. A4. Annual accumulated climatology for rainfall (m yr^{-1}) calculated using the 1980–2014 ERA-Interim daily precipitation (Dee et al. 2011). For every year of the 34-yr dataset, precipitation is first accumulated over one calendar year. Then the average is calculated.
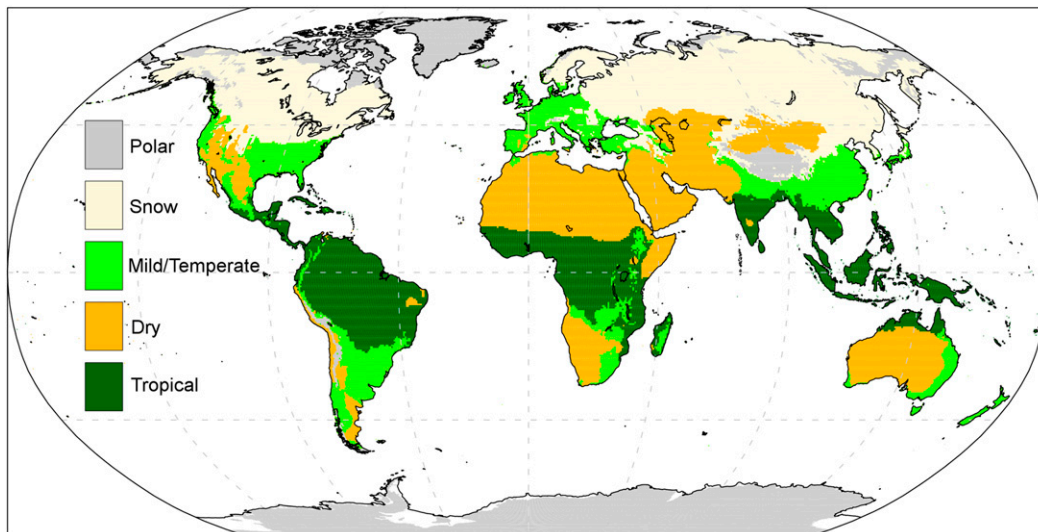
FIG. A5. World climatic classes used in the GEFF system are based on the W. Köppen classification with the following mapping conversion: class 4 (wet) to tropical, class 3 (humid) to mild/temperate, class 2 (subarctic) to snow, and class 1 (arid/semiarid) to dry.

resolution everywhere except in Greenland where the Kort-og Matrikelstyrelsen (KMS) DEM also at 30-s resolution is used.[A1] The orographic high-resolution map is also used to derive the land–sea mask, which provides the percentage of grid box covered by land. The GEFF model converts this parameter into a mask where grid points that have more than zero land are considered as land points. This is a very conservative approach that nevertheless allows the inclusions of all coastal points and small islands into the fire danger calculations.

The orography slope is an important factor to characterize fire danger behavior. This parameter is calculated at the model target resolution from the high-resolution GTOPO30 orographic dataset (Baines and Palmer 1990; Lott and Miller 1997). The slope value in IFS is transformed into slope classes as in NFDRS implementation (Cohen and Deeming 1985) following a simple linear rescaling (Fig. A3).

c. Vegetation cover

The vegetation cover is an additional mask to exclude points with no vegetation from the fire danger calculation. In IFS, vegetation is represented by six climatological parameters: vegetation cover of low vegetation, vegetation

cover of high vegetation, low vegetation type, high vegetation type, leaf area index for low vegetation, and leaf area index for high vegetation. These parameters are built from the Global Land Cover Characteristics (GLCC) dataset, which was derived from 1 year of Advanced Very High Resolution Radiometer (AVHRR) data, digital elevation models, ecoregions, and map data (Loveland et al. 2000). The nominal resolution is 1 km, and the data come on a Goode homolosine global projection. In GEFF, the fractional covers for low and high vegetation are summed to obtain a total vegetation cover. Following a conservative approach, any point with vegetation cover greater than zero is assigned vegetation mask true.

d. Mean cumulative annual precipitation

One of the inputs needed in the calculation of the Keetch–Byram drought index is the climatological total annual expected precipitation in a location. The Keetch–Byram drought index (Keetch and Byram 1968) is essentially a bookkeeping record of water deficiency in the soil. In these terms it describes anomalies relative to a defined mean state. Therefore, to avoid inconsistency (biases) between the background status defined by the expected climatological rain availability and what is predicted daily by the forecast, all terms of the water balance at the surface should be derived in a consistent way. The annual accumulated climatology for rainfall is therefore calculated using the 1980–2014 ERA-Interim (Dee et al. 2011) daily dataset by first accumulating the precipitation over every year and then calculating the average (Fig. A4).

[A1] The GTOPO30 dataset, as used in the IFS, was completed in 1996 through a collaborative effort led by the U.S. Geological Survey Earth Resources Observation and Science Center (https://lta.cr.usgs.gov/GTOPO30) and was derived from a variety of information sources. Extensive information can be found in ECMWF (2014).
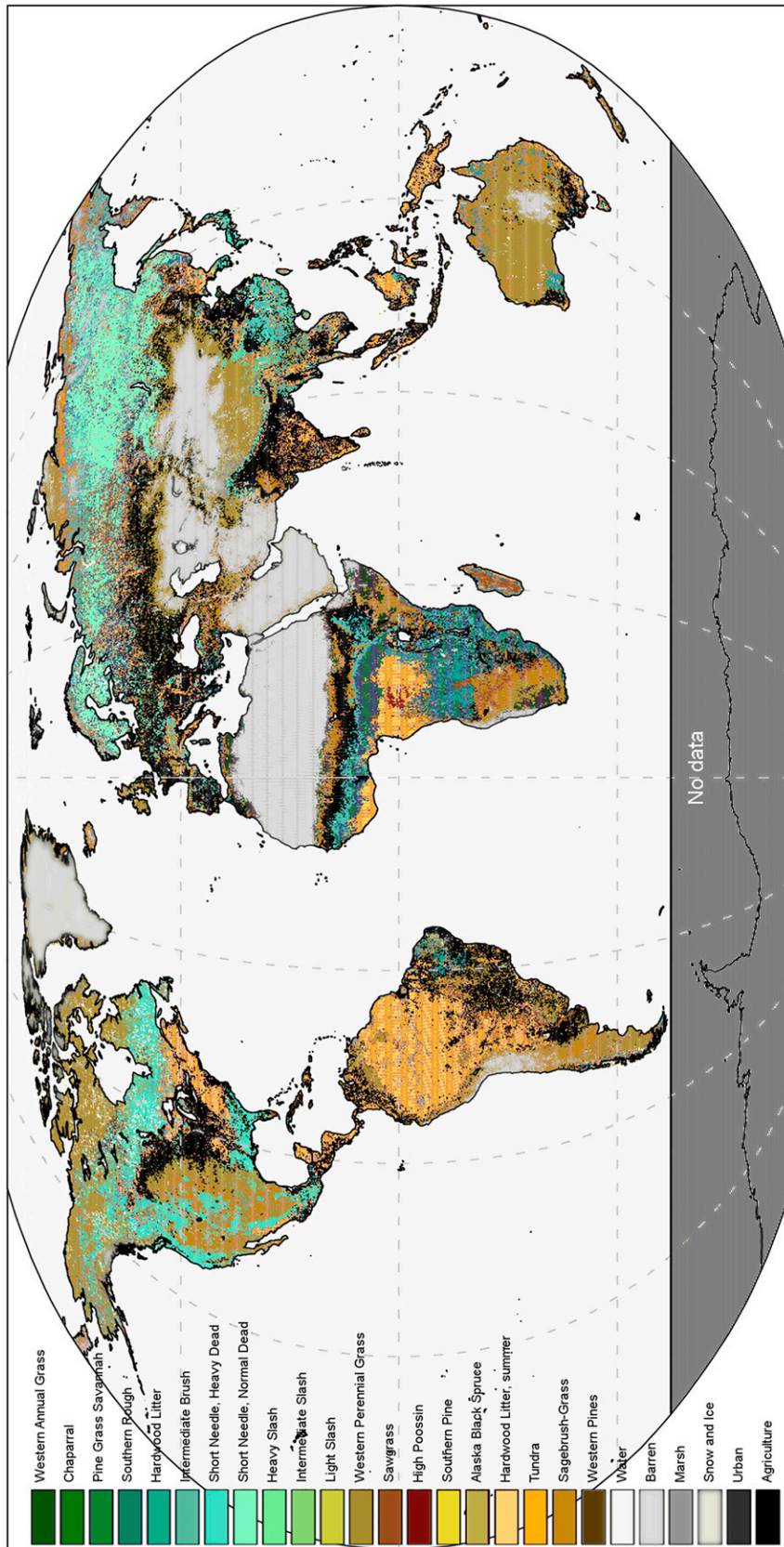
FIG. A6. Fuel-type classification used in the GEFF system. The dataset is a combination of the GLC2000 database (Bartholomé and Belward 2005) and related regional products for Africa (Mayaux et al. 2004), Asia (Bartalev et al. 2002, 2003), and Europe.

e. Climatic classification

In the NFDRS, the response of fuel moisture to environmental conditions is influenced by the mean climate. Therefore, a climate class must be specified for each grid point. In the 1978 implementation of the NFDRS (Deeming et al. 1977) four classes were used to characterize the U.S. climatic regions: 1—arid/semiarid (e.g., desert and steppe), 2—subarctic (e.g., taiga), 3—humid (e.g., forest), and 4—wet (e.g., rain forest). This classification was mostly based on the climate of temperature and precipitation in a given location, which is very similar to the approach adopted by W. Köppen for his noted world climate classification (Kottek et al. 2006; Chen and Chen 2013). To provide a numeric input to the GEFF system, we have digitalized the five class maps available in Chen and Chen (2013) with the following mapping conversion: class 4 (wet) to tropical, class 3 (humid) to mild/temperate, class 2 (subarctic) to snow, and class 1 (arid/semiarid) to dry (Fig. A5). In the polar regions, vegetation and thus fire fuel are almost negligible, and consequently the associated danger of wildfire is null. The polar climate class is therefore discarded.

f. Fuel model

The global fuel map used in the study (Fig. A6) is a product developed by JRC and derived from the Global Land Cover 2000 (GLC2000; http://forobs.jrc.ec.europa.eu/products/glc2000/glc2000.php) database (Bartholomé and Belward 2005) and related regional products for Africa (Mayaux et al. 2004), Asia (Bartalev et al. 2002, 2003), and Europe. The GLC2000 was overlaid on the NFDRS fuel models (Deeming et al. 1977; Bradshaw et al. 1983) as mapped on the conterminous United States by Burgan et al. (1998). It contains 20 vegetation species listed in Table 3 plus a series of classes for marsh, water bodies, urban, and agriculture. The derived co-occurrence matrix of NFDRS fuel models and GLC2000 land-cover classes was used as initial reference to derive, through expert judgment and interpretation, the relationships of fuel model classes with the rest of the world and regional land-cover legends. The resulting map has 1-km spatial resolution and is intended to provide a first approximation of the spatial distribution of fuel complexes throughout the world, as classified according to the NFDRS (Deeming et al. 1977; Bradshaw et al. 1983).

REFERENCES

Baines, P. G., and T. N. Palmer, 1990: Rationale for a new physically-based parametrization of subgrid scale orographic effects. ECMWF Tech. Memo. 169, 11 pp. [Available online at http://www.ecmwf.int/sites/default/files/elibrary/1990/7875-rationale-new-physically-based-parametrization-subgrid-scale-orographic-effects.pdf.]

Bartalev, S., A. Belward, D. Erchov, and A. Isaev, 2002: The land cover map of northern Eurasia: Method, product, and initial users' feedback—Global Land Cover 2000. European Commission Joint Research Centre Workshop Pres., 39 pp. [Available online at http://forobs.jrc.ec.europa.eu/products/glc2000/publications/workshop/march2002/GLC2000_march2002_bartalev.pps.]

——, ——, ——, and ——, 2003: A new SPOT4-VEGETATION derived land cover map of northern Eurasia. Int. J. Remote Sens., 24, 1977–1982, doi:10.1080/0143116031000066297.

Bartholomé, E., and A. Belward, 2005: GLC2000: A new approach to global land cover mapping from Earth observation data. Int. J. Remote Sens., 26, 1959–1977, doi:10.1080/01431160412331291297.

Boussetta, S., G. Balsamo, A. Beljaars, T. Kral, and L. Jarlan, 2013: Impact of a satellite-derived leaf area index monthly climatology in a global numerical weather prediction model. Int. J. Remote Sens., 34, 3520–3542, doi:10.1080/01431161.2012.716543.

Bradshaw, L. S., J. E. Deeming, R. E. Burgan, and J. D. Cohen, 1983: The 1978 National Fire-Danger Rating System: Technical documentation. USDA Forest Service Intermountain Forest and Range Experiment Station General Tech. Rep. INT-169, 44 pp. [Available online at http://www.fs.fed.us/rm/pubs_int/int_gtr169.pdf.]

Bradstock, R. A., J. E. Williams, and A. M. Gill, 2002: Flammable Australia: The Fire Regimes and Biodiversity of a Continent. Cambridge University Press, 462 pp.

Buizza, R., M. Miller, and T. Palmer, 1999: Stochastic representation of model uncertainties in the ECMWF ensemble prediction system. Quart. J. Roy. Meteor. Soc., 125, 2887–2908, doi:10.1002/qj.49712556006.

Burgan, R. E., 1988: 1988 revisions to the 1978 National Fire-Danger Rating System. USDA Forest Service Southeastern Forest Experiment Station Research Paper SE-273, 39 pp. [Available online at http://www.srs.fs.usda.gov/pubs/rp/rp_se273.pdf.]

——, R. W. Klaver, and J. M. Klaver, 1998: Fuel models and fire potential from satellite and surface observations. Int. J. Wildland Fire, 8, 159–170, doi:10.1071/WF9980159.

Camia, A., P. Barbosa, G. Amatulli, and J. San-Miguel-Ayanz, 2006: Fire danger rating in the European Forest Fire Information System (EFFIS): Current developments. For. Ecol. Manage., 234, S20, doi:10.1016/j.foreco.2006.08.036.

Chen, D., and H. W. Chen, 2013: Using the Köppen classification to quantify climate variation and change: An example for 1901–2010. Environ. Dev., 6, 69–79, doi:10.1016/j.envdev.2013.03.007.

Cohen, J. D., and J. E. Deeming, 1985: The National Fire-Danger Rating System: Basic equations. USDA Forest Service Pacific Southwest Forest and Range Experiment Station General Tech. Rep. PSW-82, 16 pp. [Available online at http://ftp.fs.fed.us/psw/publications/documents/psw_gtr082/psw_gtr082.pdf.]

Coles, S., J. Heffernan, and J. Tawn, 1999: Dependence measures for extreme value analyses. Extremes, 2, 339–365, doi:10.1023/A:1009963131610.

Courtier, P., J.-N. Thépaut, and A. Hollingsworth, 1994: A strategy for operational implementation of 4D-Var, using an incremental approach. Quart. J. Roy. Meteor. Soc., 120, 1367–1387, doi:10.1002/qj.49712051912.

Cruz, M. G., and M. P. Plucinski, 2007: Billo Road fire: Report on fire behaviour phenomena and suppression activities. Bushfire

Cooperative Research Centre Rep. A.07.02, 96 pp. [Available online at http://www.bushfirecrc.com/sites/default/files/managed/resource/billoroadfirefinalreportweb_0.pdf.]

Dee, D., and Coauthors, 2011: The ERA-Interim Reanalysis: Configuration and performance of the data assimilation system. *Quart. J. Roy. Meteor. Soc.*, **137**, 553–597, doi:10.1002/qj.828.

Deeming, J. E., R. E. Burgan, and J. D. Cohen, 1977: The National Fire-Danger Rating System—1978. USDA Forest Service General Tech. Rep. INTUS 39, 49 pp.

de Groot, W. J., A. S. Cantin, M. D. Flannigan, A. J. Soja, L. M. Gowman, and A. Newbery, 2013: A comparison of Canadian and Russian boreal forest fire regimes. *For. Ecol. Manage.*, **294**, 23–34, doi:10.1016/j.foreco.2012.07.033.

ECMWF, 2014: Cycle 40r1. IFS Documentation. [Available online at http://www.ecmwf.int/en/forecasts/documentation-and-support/changes-ecmwf-model/cycle-40r1/cycle-40r1.]

Esty, D. C., A. Levy, C. Kim, A. de Sherbinin, T. Srebotnjak, and V. Mara, 2008: 2008 environmental performance index. Yale Center for Environmental Law & Policy, 382 pp. [Available online at http://epi.yale.edu/sites/default/files/2008_epi_report_0.pdf.]

Ferro, C. A., 2007: A probability model for verifying deterministic forecasts of extreme events. *Wea. Forecasting*, **22**, 1089–1100, doi:10.1175/WAF1036.1.

——, and D. B. Stephenson, 2011: Extremal dependence indices: Improved verification measures for deterministic forecasts of rare binary events. *Wea. Forecasting*, **26**, 699–713, doi:10.1175/WAF-D-10-05030.1.

Flannigan, M. D., and T. H. Vonder Haar, 1986: Forest fire monitoring using NOAA satellite AVHRR. *Can. J. For. Res.*, **16**, 975–982, doi:10.1139/x86-171.

——, K. A. Logan, B. D. Amiro, W. R. Skinner, and B. Stocks, 2005: Future area burned in Canada. *Climatic Change*, **72**, 1–16, doi:10.1007/s10584-005-5935-y.

——, M. A. Krawchuk, W. J. de Groot, B. M. Wotton, and L. M. Gowman, 2009: Implications of changing climate for global wildland fire. *Int. J. Wildland Fire*, **18**, 483–507, doi:10.1071/WF08187.

Giglio, L., J. Descloitres, C. O. Justice, and Y. J. Kaufman, 2003: An enhanced contextual fire detection algorithm for MODIS. *Remote Sens. Environ.*, **87**, 273–282, doi:10.1016/S0034-4257(03)00184-6.

——, I. Csiszar, and C. O. Justice, 2006: Global distribution and seasonality of active fires as observed with the Terra and Aqua Moderate Resolution Imaging Spectroradiometer (MODIS) sensors. *J. Geophys. Res.*, **111**, G02016, doi:10.1029/2005JG000142.

——, J. T. Randerson, and G. R. Werf, 2013: Analysis of daily, monthly, and annual burned area using the fourth-generation global fire emissions database (GFED4). *J. Geophys. Res. Biogeosci.*, **118**, 317–328, doi:10.1002/jgrg.20042.

Hantson, S., S. Pueyo, and E. Chuvieco, 2015: Global fire size distribution is driven by human impact and climate. *Global Ecol. Biogeogr.*, **24**, 77–86, doi:10.1111/geb.12246.

Keetch, J. J., and G. M. Byram, 1968: A drought index for forest fire control. USDA Forest Service Southeastern Forest Experiment Station Research Paper SE-38, 32 pp. [Available online at http://www.srs.fs.usda.gov/pubs/rp/rp_se038.pdf?.]

Knote, C., G. Bonafe, and F. Di Giuseppe, 2009: Leaf area index specification for use in mesoscale weather prediction systems. *Mon. Wea. Rev.*, **137**, 3535–3550, doi:10.1175/2009MWR2891.1.

Kottek, M., J. Grieser, C. Beck, B. Rudolf, and F. Rubel, 2006: World map of the Köppen-Geiger climate classification updated. *Meteor. Z.*, **15**, 259–263, doi:10.1127/0941-2948/2006/0130.

Lott, F., and M. J. Miller, 1997: A new subgrid-scale orographic drag parametrization: Its formulation and testing. *Quart. J. Roy. Meteor. Soc.*, **123**, 101–127, doi:10.1002/qj.49712353704.

Loveland, T., B. Reed, J. Brown, D. Ohlen, Z. Zhu, L. Yang, and J. Merchant, 2000: Development of a global land cover characteristics database and IGBP discover from 1 km AVHRR data. *Int. J. Remote Sens.*, **21**, 1303–1330, doi:10.1080/014311600210191.

Luke, R. H., and A. G. McArthur, 1978: *Bushfires in Australia*. Australian Government Publishing Service, 359 pp.

Mayaux, P., E. Bartholomé, S. Fritz, and A. Belward, 2004: A new land-cover map of Africa for the year 2000. *J. Biogeogr.*, **31**, 861–877, doi:10.1111/j.1365-2699.2004.01073.x.

McArthur, A. G., 1966: Weather and grassland fire behaviour. Forestry and Timber Bureau Leaflet 100, 23 pp.

——, 1967: Fire behaviour in eucalypt forests. Forestry and Timber Bureau Leaflet 107, 36 pp.

Mölders, N., 2008: Suitability of the Weather Research and Forecasting (WRF) model to predict the June 2005 fire weather for interior Alaska. *Wea. Forecasting*, **23**, 953–973, doi:10.1175/2008WAF2007062.1.

——, 2010: Comparison of Canadian Forest Fire Danger Rating System and National Fire Danger Rating System fire indices derived from Weather Research and Forecasting (WRF) Model data for the June 2005 interior Alaska wildfires. *Atmos. Res.*, **95**, 290–306, doi:10.1016/j.atmosres.2009.03.010.

Myneni, R., and Coauthors, 2002: Global products of vegetation leaf area and fraction absorbed PAR from year one of MODIS data. *Remote Sens. Environ.*, **83**, 214–231, doi:10.1016/S0034-4257(02)00074-3.

Noble, I. R., G. A. V. Bary, and A. M. Gill, 1980: McArthur's fire-danger meters expressed as equations. *Aust. J. Ecol.*, **5**, 201–203, doi:10.1111/j.1442-9993.1980.tb01243.x.

Pausas, J. G., and S. Paula, 2012: Fuel shapes the fire–climate relationship: Evidence from Mediterranean ecosystems. *Global Ecol. Biogeogr.*, **21**, 1074–1082, doi:10.1111/j.1466-8238.2012.00769.x.

Preisler, H. K., D. R. Brillinger, R. E. Burgan, and J. Benoit, 2004: Probability based models for estimation of wildfire risk. *Int. J. Wildland Fire*, **13**, 133–142, doi:10.1071/WF02061.

——, R. E. Burgan, J. C. Eidenshink, J. M. Klaver, and R. W. Klaver, 2009: Forecasting distributions of large federal-lands fires utilizing satellite and gridded weather information. *Int. J. Wildland Fire*, **18**, 508–516, doi:10.1071/WF08032.

Roads, J., F. Fujioka, S. Chen, and R. Burgan, 2005: Seasonal fire danger forecasts for the USA. *Int. J. Wildland Fire*, **14**, 1–18, doi:10.1071/WF03052.

San-Miguel-Ayanz, J., J. Carlson, M. Alexander, K. Tolhurst, G. Morgan, R. Sneeuwjagt, and M. Dudley, 2003: Current methods to assess fire danger potential. *Wildland Fire Danger Estimation and Mapping: The Role of Remote Sensing Data*, E. Chuvieco, Ed., Series in Remote Sensing, Vol. 4., World Scientific Publishing, 21–61 pp.

Schroeder, W., E. Prins, L. Giglio, I. Csiszar, C. Schmidt, J. Morisette, and D. Morton, 2008: Validation of GOES and MODIS active fire detection products using ASTER and ETM+ data. *Remote Sens. Environ.*, **112**, 2711–2726, doi:10.1016/j.rse.2008.01.005.

Stephenson, D., B. Casati, C. Ferro, and C. Wilson, 2008: The extreme dependency score: A non-vanishing measure for forecasts of rare events. *Meteor. Appl.*, **15**, 41–50, doi:10.1002/met.53.

Stocks, B. J., T. Lynham, B. Lawson, M. Alexander, C. Van Wagner, R. McAlpine, and D. Dube, 1989: Canadian forest fire danger rating system: An overview. *For. Chron.*, **65**, 258–265, doi:10.5558/tfc65258-4.

——, and Coauthors, 2002: Large forest fires in Canada, 1959–1997. *J. Geophys. Res.*, **107**, 8149, doi:10.1029/2001JD000484.

Swaine, M., 1992: Characteristics of dry forest in West Africa and the influence of fire. *J. Veg. Sci.*, **3**, 365–374, doi:10.2307/3235762.

Tang, Y., H. Lin, and A. M. Moore, 2008: Measuring the potential predictability of ensemble climate predictions. *J. Geophys. Res.*, **113**, D04108, doi:10.1029/2007JD008804.

Taylor, S. W., and M. E. Alexander, 2006: Science, technology, and human factors in fire danger rating: The Canadian experience. *Int. J. Wildland Fire*, **15**, 121–135, doi:10.1071/WF05021.

Van Wagner, C. E., 1974: Structure of the Canadian forest fire weather index. Canadian Forestry Service Publ. 1333, 44 pp. [Available online at http://www.cfs.nrcan.gc.ca/bookstore_pdfs/24864.pdf.]

——, 1987: Development and structure of the Canadian Forest Fire Weather Index System. Canadian Forestry Service Tech. Rep. 35, 37 pp. [Available online at http://cfs.nrcan.gc.ca/pubwarehouse/pdfs/19927.pdf.]

——, and T. L. Pickett, 1985: Equations and FORTRAN program for the Canadian Forest Fire Weather Index System. Canadian Forestry Service Tech. Rep. 33, 18 pp. [Available online at http://cfs.nrcan.gc.ca/pubwarehouse/pdfs/19973.pdf.]

Wastl, C., C. Schunk, M. Lüpke, G. Cocca, M. Conedera, E. Valese, and A. Menzel, 2013: Large-scale weather types, forest fire danger, and wildfire occurrence in the Alps. *Agric. For. Meteor.*, **168**, 15–25, doi:10.1016/j.agrformet.2012.08.011.

Westerling, A. L., H. G. Hidalgo, D. R. Cayan, and T. W. Swetnam, 2006: Warming and earlier spring increase western U.S. forest wildfire activity. *Science*, **313**, 940–943, 313, doi:10.1126/science.1128834.

Wooster, M., B. Zhukov, and D. Oertel, 2003: Fire radiative energy for quantitative study of biomass burning: Derivation from the bird experimental satellite and comparison to MODIS fire products. *Remote Sens. Environ.*, **86**, 83–107, doi:10.1016/S0034-4257(03)00070-1.